

Quantum Theory for Large Molecules C_{60} Diffraction

Xiang-Yao Wu^a *, Bai-Jun Zhang^a, Xiao-Jing Liu^a, Nuo Ba^a

Yi-Heng Wu^a, Hou-Li Tang^a, Jing Wang^a and Si-Qi Zhang^a

a. Institute of Physics, Jilin Normal University, Siping 136000, China

Diffraction phenomena of large molecules have been studied in many experiments, and these experiments are described by many theoretical works. In this paper, we study C_{60} molecules single and double-slit diffraction with quantum theory approach, and we pay close attention to the C_{60} diffraction experiment carried out by A. Zeilinger et al in 1999. In double-slit diffraction, we consider the decoherence effect, and find the theoretical results are in good agreement with experimental data.

PACS: 03.75.Dg, 03.65.Ta, 03.65.Yz

Keywords: C_{60} diffraction; Quantum theory; Decoherence effect

1. Introduction

As is well known, the matter-wave diffraction has become a large field of interest over the last years, and it is extended to electron, neutron, C_{60} , atom, more massive, complex objects, like large molecules I_2 , C_{60} and C_{70} , which were found in experiments [1-5]. At present, There are classical and quantum methods to study interference and diffraction [6-12]. The classical optics with its standard wave-theoretical methods and approximations, in particular those of Huygens and Kirchhoff, has been successfully applied to classical optics, and has yielded good agreement with many experiments. This simple wave-optical approach also gives a description of matter wave diffraction. However, matter-wave interference and diffraction are quantum phenomena, and its full description needs quantum mechanical approach. Recently, there are some quantum theory approach to study electron and C_{60} diffraction, and obtain some important and new results [13-17]. In this paper, we study the C_{60} single and double-slit diffraction with the quantum approach, and compare to the C_{60} diffraction ($\lambda \approx 250\text{\AA}$) carried out by A. Zeilinger *et. al* in 1999 [18]. The results we obtained are shown in Fig. 3, Fig. 4 and Fig. 5. In view of quantum mechanics, the C_{60} has the nature of wave, and the wave is described by wave function $\psi(\vec{r}, t)$, and the wave function $\psi(\vec{r}, t)$ has statistical meaning, i.e., $|\psi(\vec{r}, t)|^2$ can be explained as particle's probability density. For the C_{60} slit diffraction, if we can calculate the C_{60} wave function $\psi(\vec{r}, t)$ distributing on display screen, we can obtain the diffraction intensity of C_{60} molecules, since the diffraction intensity is directly proportional to $|\psi(\vec{r}, t)|^2$. In the slit diffraction, the C_{60} wave functions can be divided into three parts. The first is the incident area, and the C_{60} wave function is a plane wave. The second is the slit area, where the C_{60} wave function can be calculated by the Schrödinger wave equation. The third is the diffraction area, where the C_{60} wave function can be obtained by path integral. In the following, we shall calculate these wave functions. Finally, we study the decoherence effect in the C_{60} double slit diffraction. The decoherence effect is important for the large molecules diffraction, and the result is in agreement with the experiment data.

* E-mail: wuxy2066@163.com

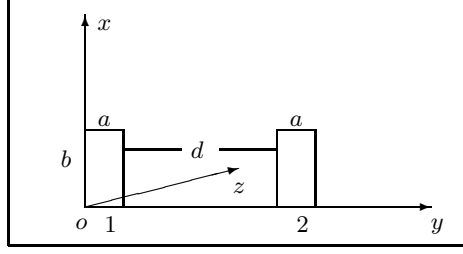


FIG. 1: Double-slit geometry with a the slit width, b the slit length and d the distance between the two slits.

2. Quantum approach of C_{60} diffraction

In an infinite plane, we consider a double-slit, its width a , length b and the slit-to-slit distance d are shown in FIG. 1. The x axis is along the slit length b and the y axis is along the slit width a . We calculate the C_{60} wave function in the first single slit (left) with the Schrödinger equation, and the C_{60} wave function of the second single slit (right) can be obtained easily. At time t , we suppose that the incident plane wave travels along the z axis. It is

$$\psi_0(z, t) = A e^{\frac{i}{\hbar}(pz - Et)}, \quad (1)$$

where A is plane wave amplitude.

The potential in the first single slit is

$$V(x, y, z) = \begin{cases} 0 & 0 \leq x \leq b, 0 \leq y \leq a, 0 \leq z \leq c, \\ \infty & \text{otherwise,} \end{cases} \quad (2)$$

where c is the thickness of the single slit. The time-dependent and time-independent Schrödinger equations are

$$i\hbar \frac{\partial}{\partial t} \psi(\vec{r}, t) = -\frac{\hbar^2}{2M} \left(\frac{\partial^2}{\partial x^2} + \frac{\partial^2}{\partial y^2} + \frac{\partial^2}{\partial z^2} \right) \psi(\vec{r}, t), \quad (3)$$

$$\frac{\partial^2 \psi(\vec{r})}{\partial x^2} + \frac{\partial^2 \psi(\vec{r})}{\partial y^2} + \frac{\partial^2 \psi(\vec{r})}{\partial z^2} + \frac{2ME}{\hbar^2} \psi(\vec{r}) = 0, \quad (4)$$

where $M(E)$ is the mass(energy) of the C_{60} . The relation between $\psi(\vec{r}, t)$ and $\psi(\vec{r})$ is

$$\psi(\vec{r}_1, \vec{r}_2 \cdots \vec{r}_N, t) = \psi(\vec{r}_1, \vec{r}_2 \cdots \vec{r}_N) g(t). \quad (5)$$

The Eq. (19) become as

In Eq. (4), the wave function $\psi(x, y, z)$ satisfies the boundary conditions

$$\psi(0, y, z) = \psi(b, y, z) = 0, \quad (6)$$

$$\psi(x, 0, z) = \psi(x, a, z) = 0. \quad (7)$$

The partial differential Eq. (4) can be solved by the method of separation of variable. By writing

$$\psi(x, y, z) = X(x)Y(y)Z(z). \quad (8)$$

The general solution of Eq. (3) is

$$\begin{aligned}\psi_1(x, y, z, t) &= \sum_{mn} \psi_{mn}(x, y, z, t) \\ &= \sum_{mn} D_{mn} \sin \frac{n\pi x}{b} \sin \frac{m\pi y}{a_1} e^{i\sqrt{\frac{2ME}{\hbar^2} - \frac{n^2\pi^2}{b^2} - \frac{m^2\pi^2}{a_1^2}}z} e^{-\frac{i}{\hbar}Et}.\end{aligned}\quad (9)$$

Equation (9) is the C_{60} wave function in the first single slit. Since the wave functions are continuous at $z = 0$, we have

$$\psi_0(x, y, z, t) |_{z=0} = \psi_1(x, y, z, t) |_{z=0}, \quad (10)$$

from Eqs. (2), (6) and (9), we can obtain the Fourier coefficient D_{mn} by Fourier transform

$$\begin{aligned}D_{mn} &= \frac{4}{a_1 b} \int_0^{a_1} \int_0^b A \sin \frac{n\pi\xi}{b} \sin \frac{m\pi\eta}{a_1} d\xi d\eta \\ &= \begin{cases} \frac{16A}{mn\pi^2} & m, n, \text{ odd}, \\ 0 & \text{otherwise}, \end{cases}\end{aligned}\quad (11)$$

substituting Eq. (11) into Eq. (9), we can obtain the C_{60} wave function in the first single slit.

$$\begin{aligned}\psi_1(x, y, z, t) &= \sum_{m,n=0}^{\infty} \frac{16A}{(2m+1)(2n+1)\pi^2} \sin \frac{(2n+1)\pi x}{b} \sin \frac{(2m+1)\pi y}{a} \\ &\cdot e^{i\sqrt{\frac{2ME}{\hbar^2} - \frac{(2n+1)^2\pi^2}{b^2} - \frac{(2m+1)^2\pi^2}{a^2}}z} e^{-\frac{i}{\hbar}Et}.\end{aligned}\quad (12)$$

The C_{60} wave function in the second single slit can be obtained by making the coordinate translations $x' = x$, $y' = y - a - d$, $z' = z$, and we can obtain the C_{60} wave function $\psi_2(x, y, z, t)$ in the second slit

$$\begin{aligned}\psi_2(x, y, z, t) &= \sum_{m,n=0}^{\infty} \frac{16A}{(2m+1)(2n+1)\pi^2} \sin \frac{(2n+1)\pi x}{b} \sin \frac{(2m+1)\pi(y-a-d)}{a} \\ &\cdot e^{i\sqrt{\frac{2ME}{\hbar^2} - \frac{(2n+1)^2\pi^2}{b^2} - \frac{(2m+1)^2\pi^2}{a^2}}z} e^{-\frac{i}{\hbar}Et}.\end{aligned}\quad (13)$$

3. The wave function of C_{60} diffraction

With the approach of path integral, we can calculate C_{60} wave function in the diffraction area.

The diffraction area is shown in FIG. 2, where \mathbf{r}_0 is the position of point $P_0(x_0, y_0, c)$ on the slit surface ($z = c$), $P(x, y, z)$ is an arbitrary point in the diffraction area. From Eq. (12), we can obtain the wave function in slit surface ($z = c$)

$$\begin{aligned}\psi_{P_0}(x, y, z, t) &= \sum_{m,n=0}^{\infty} \frac{16A}{(2m+1)(2n+1)\pi^2} \sin \frac{(2n+1)\pi x_0}{b} \sin \frac{(2m+1)\pi y_0}{a} \\ &\cdot e^{i\sqrt{\frac{2ME}{\hbar^2} - \frac{(2n+1)^2\pi^2}{b^2} - \frac{(2m+1)^2\pi^2}{a^2}}c} e^{-\frac{i}{\hbar}Et_0}.\end{aligned}\quad (14)$$

The diffraction wave function ψ_{out} on the point $P(x, y, z)$ can be calculated by the formula of path integral [17]

$$\psi_P(\mathbf{r}, t) = \int K(\mathbf{r}, t; \mathbf{r}_0, t_0) \psi_{P_0}(\mathbf{r}_0, t_0) dx_0 dy_0, \quad (15)$$

where $K(\mathbf{r}, t; \mathbf{r}_0, t_0)$ is the C_{60} molecules propagator, it is

$$K(\mathbf{r}, t; \mathbf{r}_0, t_0) = \left(\frac{M}{2\pi i \hbar (t - t_0)} \right)^{\frac{3}{2}} \exp \left[\frac{iMR^2}{2\hbar(t - t_0)} \right], \quad (16)$$

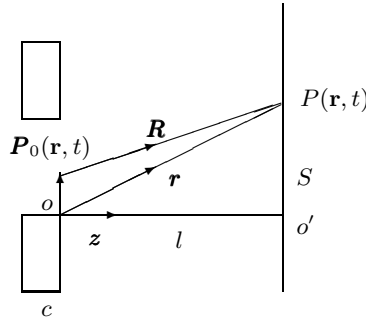


FIG. 2: Diffraction area of the single slit

where M is the mass of C_{60} molecules, and R is the distance between point P_0 and point P , it is

$$\begin{aligned} R &= \sqrt{|\mathbf{r} - \mathbf{r}_0|^2} = \sqrt{(x - x_0)^2 + (y - y_0)^2 + (z - c)^2} \\ &= \sqrt{x^2 + y^2 + z^2 + x_0^2 + y_0^2 + c^2 - 2xx_0 - 2yy_0 - 2zc}. \end{aligned} \quad (17)$$

Assume that the angle between \mathbf{r} and x axis (y axis) is $\frac{\pi}{2} - \alpha$ ($\frac{\pi}{2} - \beta$), and then α (β) is the angle between \mathbf{r} and the surface of $yz(xz)$. we obtain

$$\begin{aligned} R^2 &= x^2 + y^2 + z^2 + x_0^2 + y_0^2 + c^2 - 2xx_0 - 2yy_0 - 2zc \\ &= r^2 - 2r \sin \alpha x_0 - 2r \sin \beta y_0 + x_0^2 + y_0^2 \\ &\approx r^2 - 2r \sin \alpha x_0 - 2r \sin \beta y_0, \end{aligned} \quad (18)$$

where $r^2 = x^2 + y^2 + (z - c)^2$, In Eq. (18), the terms x_0^2 and y_0^2 can be neglected. Substituting Eqs. (14), (16), (18) into (15) yields

$$\begin{aligned} \psi_P(\mathbf{r}, t) &= e^{\frac{iMr^2}{2\hbar(t-t_0)}} \left(\frac{M}{2\pi i \hbar(t-t_0)} \right)^{\frac{3}{2}} \sum_{m=0}^{\infty} \sum_{n=0}^{\infty} \frac{16A}{(2m+1)(2n+1)\pi^2} \\ &\cdot e^{i\sqrt{\frac{2ME}{\hbar^2} - \left(\frac{(2n+1)\pi}{b}\right)^2 - \left(\frac{(2m+1)\pi}{a_1}\right)^2} \cdot c} \\ &\int_0^b e^{\frac{-iMr \sin \alpha x_0}{\hbar(t-t_0)}} \sin \frac{(2n+1)\pi x_0}{b} dx_0 \int_0^a e^{\frac{-iMr \sin \beta y_0}{\hbar(t-t_0)}} \sin \frac{(2m+1)\pi y_0}{a} dy_0. \end{aligned} \quad (19)$$

With de Broglie relationship $p = \hbar k = \frac{\hbar}{\lambda}$, there is

$$k = \frac{Mv}{\hbar}, \quad (20)$$

where $v = \frac{R}{t-t_0}$, thus

$$k = \frac{MR}{\hbar(t-t_0)} \approx \frac{Mr}{\hbar(t-t_0)}, \quad (21)$$

then

$$\left(\frac{M}{2\pi i \hbar(t-t_0)} \right)^{\frac{3}{2}} = \left(\frac{Mr}{2\pi i \hbar(t-t_0)r} \right)^{\frac{3}{2}} = \left(-\frac{\sqrt{2}}{2} - \frac{\sqrt{2}}{2}i \right) \left(\frac{k}{2\pi r} \right)^{\frac{3}{2}}, \quad (22)$$

and

$$e^{\frac{iMr^2}{2\hbar(t-t_0)}} \approx e^{\frac{ikr}{2}}, \quad (23)$$

and so

$$\begin{aligned} \psi_{1P}(\mathbf{r}, t) &= \left(-\frac{\sqrt{2}}{2} - \frac{\sqrt{2}}{2}i \right) \left(\frac{k}{2\pi r} \right) \sqrt{\frac{k}{2\pi r}} e^{\frac{ikr}{2}} \sum_{m=0}^{\infty} \sum_{n=0}^{\infty} \frac{16A}{(2m+1)(2n+1)\pi^2} \\ &\cdot e^{i\sqrt{\frac{2ME}{\hbar^2} - \left(\frac{(2n+1)\pi}{b}\right)^2 - \left(\frac{(2m+1)\pi}{a_1}\right)^2} \cdot c} \\ &\int_0^b e^{-ik \sin \alpha x_0} \sin \frac{(2n+1)\pi x_0}{b} dx_0 \int_0^a e^{-ik \sin \beta y_0} \sin \frac{(2m+1)\pi y_0}{a} dy_0. \end{aligned} \quad (24)$$

Equation (24) is the C_{60} diffraction wave function of the first slit, and the diffraction wave function ψ_{2P} for the second slit can be obtained by making the coordinate translations $x' = x, y' = y - (a + d), z' = z$, it is

$$\begin{aligned} \psi_{2P}(x, y, z, t) = & -\frac{e^{ikR}}{4\pi R} e^{-\frac{i}{\hbar}Et} \sum_{m=0}^{\infty} \sum_{n=0}^{\infty} \frac{16A}{(2m+1)(2n+1)\pi^2} e^{i\sqrt{\frac{2ME}{\hbar^2} - (\frac{(2n+1)\pi}{b})^2 - (\frac{(2m+1)\pi}{a})^2} \cdot c} \\ & [i\sqrt{\frac{2ME}{\hbar^2} - (\frac{(2n+1)\pi}{b})^2 - (\frac{(2m+1)\pi}{a})^2} + (ik - \frac{1}{R})\sqrt{\cos^2 \alpha - (\frac{s}{R})^2}] \\ & \int_0^b e^{-ik \sin \alpha \cdot x'} \sin \frac{(2n+1)\pi}{b} x' dx' \\ & \int_{a+d}^{2a+d} e^{-ik \sin \beta \cdot y'} \sin \frac{(2m+1)\pi}{a} (y' - (a+d)) dy', \end{aligned} \quad (25)$$

where d is the two slit distance. The total diffraction wave function for the double-slit is

$$\psi_P(x, y, z, t) = c_1 \psi_{1P}(x, y, z, t) + c_2 \psi_{2P}(x, y, z, t), \quad (26)$$

where c_1 and c_2 are superposition coefficients, and $|c_1|^2 + |c_2|^2 = 1$. For the C_{60} single-slit diffraction, we can obtain the relative diffraction intensity I on the display screen,

$$I \propto |\psi_{1P}(x, y, z, t)|^2. \quad (27)$$

For the C_{60} double-slit diffraction, we can obtain the relative diffraction intensity I on the display screen,

$$\begin{aligned} I & \propto |\psi_P(x, y, z, t)|^2 \\ & = c_1^2 |\psi_{1P}(x, y, z, t)|^2 + c_2^2 |\psi_{2P}(x, y, z, t)|^2 + 2c_1 c_2 \text{Re}[\psi_{1P}^*(x, y, z, t) \psi_{2P}(x, y, z, t)]. \end{aligned} \quad (28)$$

From Eqs. (27) and (28), we can obtain the relation between diffraction intensity and diffraction angle. In Ref. [16], their experiment data is about the relation between diffraction intensity and diffraction position. The relation is

$$\sin[\beta] = \frac{s}{R} = \frac{s}{\sqrt{l^2 + s^2}}. \quad (29)$$

Where l is the distance from the slit to display screen, and s is diffraction position.

4. Decoherence effect in double-slit diffraction

Decoherence is introduced here using a simple phenomenological theoretical model that assumes an exponential damping of the interferences [7, 20, 21], i.e., the decoherence is the dynamic suppression of the interference terms owing to the interaction between system and environment. The Eq. (26) describes the coherence state coherence superposition, without considering the interaction of system with external environment. When we consider the effect of external environment, the total wave function of system and environment for the double-slit factorizes as [7]

$$\psi_{out}(x, y, z, t) = c_1 \psi_{out1} \otimes |E_1\rangle_t + c_2 \psi_{out2} \otimes |E_2\rangle_t, \quad (30)$$

where $|E_1\rangle_t$ and $|E_2\rangle_t$ describe the state of the environment. The diffraction intensity on the screen is now given by [7]:

$$I = (1 + |\alpha_t|^2)(c_1^2 |\psi_{out1}(x, y, z, t)|^2 + c_2^2 |\psi_{out2}(x, y, z, t)|^2 + 2c_1 c_2 \Lambda_t \text{Re}[\psi_{out1}^*(x, y, z, t) \psi_{out2}(x, y, z, t)]). \quad (31)$$

where $\alpha_t = \langle E_2 | E_1 \rangle_t$, and $\Lambda_t = \frac{2|\alpha_t|}{1+|\alpha_t|^2}$. Thus, Λ_t is defined as the quantum coherence degree. In Eq. (31), the two slits wave functions ψ_{1P} and ψ_{2P} are calculated by the quantum approach (in Eqs. (24)-(25)).

In Refs. [7], the two slits wave functions are two Gaussian wave packets. The fringe visibility of ν is defined as [7]:

$$\nu = \frac{I_{max} - I_{min}}{I_{max} + I_{min}}. \quad (32)$$

Where I_{max} and I_{min} are the intensities corresponding to the central maximum and the first minimum next to it, respectively. The value for the fringe visibility of $\nu = 0.50$ is obtained in Zeilinger et. al. experiment [18] ($I_{max} = 880, I_{min} = 300$), and the quantum coherence degree $\Lambda_t \approx \nu$ [7].

5. Numerical result

Next, we present our numerical calculation of relative diffraction intensity. The main input parameters are: C_{60} molecules mass $M = 1.4 \times 10^{-24}$ kg, and Planck's constant $\hbar = 1.055 \times 10^{-34}$ Js. For the single-slit experiment [18], the C_{60} velocity $v = 220$ m/s (corresponding to C_{60} wave length $\lambda = 250\text{\AA}$), the slit width $a = 10\mu\text{m}$, and the distance between slit and display screen $l = 2.29$ m. In our calculation, we take the same experiment parameters above, and the theoretical input amplitude parameters are: $A = 2.87 \times 10^{14}$, the diffraction angle on yz surface $\alpha = 0$ rad, the slit length $b = 0.01$ m and the slit thickness $c = 1.3\mu\text{m}$. From Eq. (27), we can obtain the single slit diffraction intensity pattern, and it is shown in FIG. 3. In FIG. 3, the solid curve is our calculation result, and the dot curve is the experiment data [18]. From FIG. 3, we can find the calculation result is agreement with experiment data. For the double-slit diffraction, we consider two cases: coherence superposition and decoherence effect. For coherence superposition, from Eq. (28), we can calculate the diffraction intensity and it is shown in FIG. 4. The experiment parameters are: the C_{60} wavelength $\lambda = 250\text{\AA}$, the first and second slit width, $a = 0.05\mu\text{m}$, the distance between the two slit $d = 0.05\mu\text{m}$, the slit thickness $c = 1.3\mu\text{m}$, the distance between slit and display screen $l = 1.25$ m. In our calculation, we take the same experiment parameters above, and the theoretical input parameters are superposition coefficients $c_1 = 0.566, c_2 = 0.824$ ($|c_1|^2 + |c_2|^2 = 1$) and amplitude parameter $A = 1.27 \times 10^{22}$. In FIG. 4, the solid curve is our theoretical calculation, and the dot curve is the experiment data [18]. From the FIG. 4, we find that the theoretical result is in accordance with the experiment data, when the position s is in the range of $|s| \geq 100\mu\text{m}$. When the position s is in the range of $|s| \leq 100\mu\text{m}$, the theoretical result has a large discrepancy with the experiment data. We find the discrepancy can be eliminated when the decoherence effect is considered. From Eq. (31), we can obtain the diffraction intensity pattern and it is shown in FIG. 5. In calculation, superposition coefficients $c_1 = 0.565, c_2 = 0.824$, amplitude $A = 1.69 \times 10^{22}$ and quantum coherence degree $\Lambda_t = 0.50$. From FIG. 5, we can find that the new calculation result is more improvement than it in FIG. 4, and it is in accordance with the experiment data, i.e., when the decoherence effect is considered, the discrepancy between the theoretical result and experiment data can be eliminated.

6. Conclusion

In conclusion, we study C_{60} single and double-slit diffraction with quantum theory approach. The theoretical result of single-slit is in accordance with the experiment data. For the double-slit diffraction, we study the diffraction intensity by two approaches, which are the coherence superposition and decoherence mechanism. When we only consider the superposition of coherence, we find the theoretical result has a large discrepancy with the experiment data, and when we consider the decoherence mechanism, we find the theoretical result is in accordance with the experiment data. So, the decoherence mechanism is important for the double-slit diffraction of the large molecules. We think the new quantum theory approach has universal applicability, such as, it can study electron, atom and molecular diffraction, and it can also be studied multi-slit and grating diffraction.

-
- ¹ O. Carnal and J. Mlynek, Phys. Rev. Lett. **66** 2689 (1991).
 - ² John D. Perreault and Alexander D. Cronin Phys. Rev A **71**, 053612 (2005).
 - ³ Atomic, Molecular, and Optical Physics: Atoms and Molecules, edited by F. B. Dunning and R. G. Hulet sAcademic, New York, (1996).
 - ⁴ O. Nairz, M. Arudt and A. Zeilinger, J. Mod. Opt. **47** 2811 (2000).
 - ⁵ Kunze S, Dieckmann k and Rempe G, Phys. Rev. Lett. **78** 2038 (1997).
 - ⁶ B. Brezger, L. Hackermuller, S. Uttenthaler, J. Petschinka, M. Arndt and A. Zeilinger, Phys. Rev. Lett. **88**, 100404 (2002).
 - ⁷ S. A. Sanz, F. Borondo and J. M. Bastiaans, Phys. Rev. A **71**, 042103 (2005).
 - ⁸ O. Carnal and J. Mlynek, Phys. Rev. Lett. **66**, 2689 (1991)
 - ⁹ W. Schöllkopf and P. J. Toennies, Science **266**, 1345 (1994).
 - ¹⁰ A. Zeilinger, R. Gahler, W. Treimer, and W. Mampe, Rev. Mod. Phys. **60**, 1067 (1988).
 - ¹¹ O. Nairz, M. Arudt and A. Zeilinger, J. Mod. Opt. **47**, 2811 (2000).
 - ¹² S. Kunze, K. Dieckmann and G. Rempe, Phys. Rev. Lett. **78**, 2038 (1997).
 - ¹³ Xiang-Yao WuBai-Jun ZhangXiao-Jing Liu, FIZIKA B (Zagreb) 18, 195 (2009).
 - ¹⁴ Li Wang, Bai-Jun Zhang, Zhong Hua, Ji Li, Xiao-Jing Liu and Xiang-Yao Wu, Progress of Theoretical Physics 121685 (2009).
 - ¹⁵ Xiang-Yao Wu, Bai-Jun Zhang, Li-Xin Chi, Jing-Hai Yang, Xiao-Jing Liu and Yi-Heng Wu, J. Mod. Opt. 49 2082 (2010).
 - ¹⁶ A. Viale, M. Vicari and N. Zanghi, Phys. Rev. A **68**, 063610 (2003).
 - ¹⁷ R. Tumulka, A. Viale and N. Zanghi, Phys. Rev. A **75**, 055602 (2007).
 - ¹⁸ M. Arudt, O. Nairz, J. Vos-Andreae, C. Kwller, G. Vander Zouw and A. Zeilinger, Nature **401** 680 (1999).
 - ¹⁹ R. Tumulka, A. Viale and N. Zanghi, Phys. Rev. A **75**, 055602 (2007).
 - ²⁰ C. Kiefer and E. Joos, Decoherence: Concepts and Examples, in Quantum Future, eds. P. Blanchard and A. Jadczyk (Springer, Berlin, 1998).
 - ²¹ E. Joos and H.D. Zeh, Zeit. Phys. **59B**, 223 (1985).

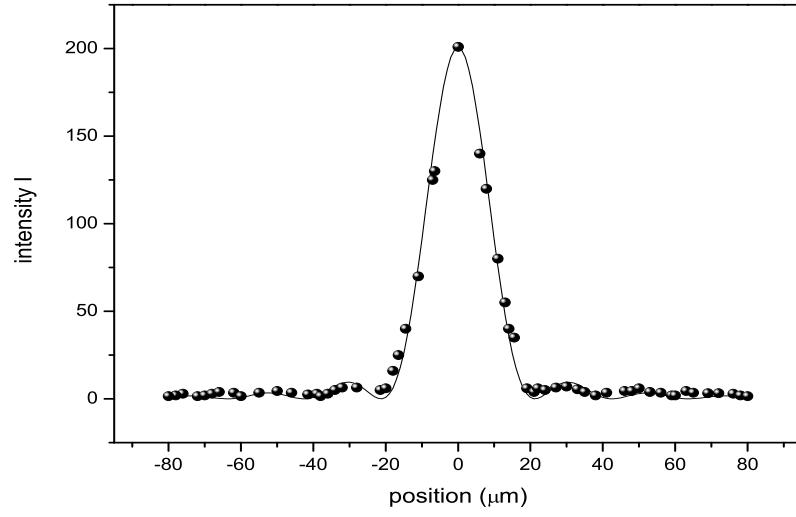


FIG. 3: Comparison between theoretical prediction from Eq. (27) (solid line) and experimental data taken from [18](circle point) for C_{60} single-slit diffraction.

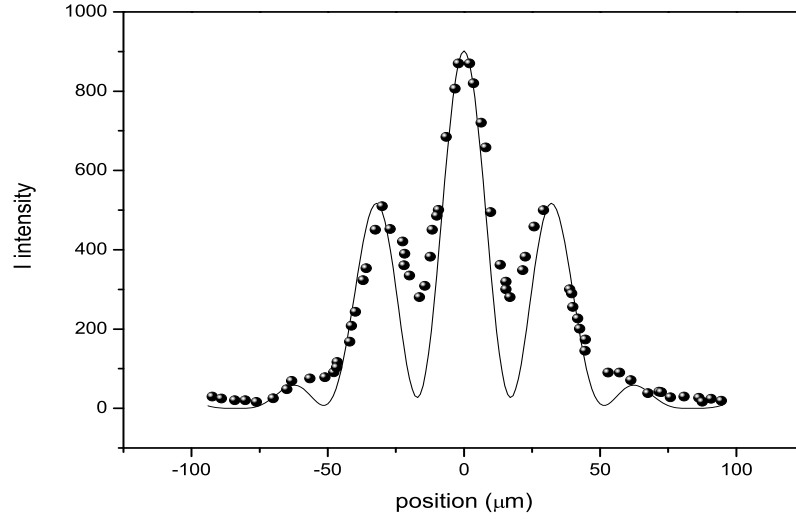


FIG. 4: Comparison between theoretical prediction from Eq. (28) (solid line) and experimental data taken from [18](circle point) for C_{60} double-slit diffraction, no including the decoherence effects

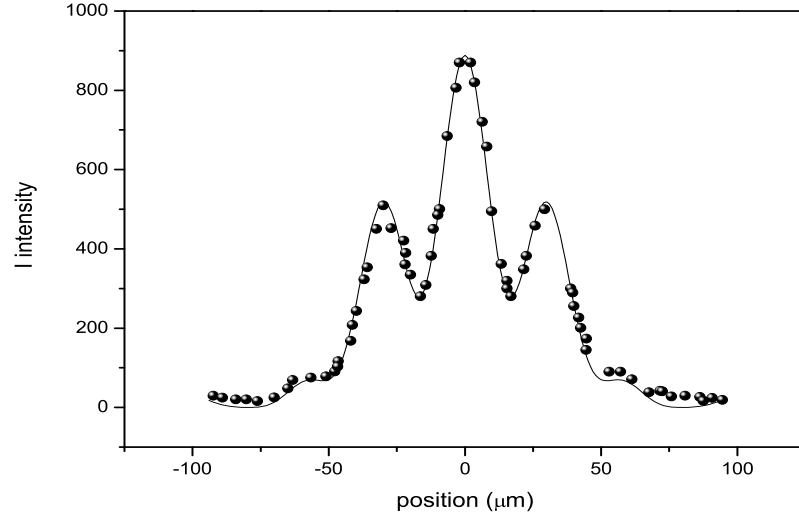


FIG. 5: Comparison between theoretical prediction from Eq. (31) (solid line) and experimental data taken from [18](circle point) for C_{60} double-slit diffraction, including the decoherence effects.